

## Title: The Use of Optical Emission Spectroscopy to Solve Manufacturing Scaling Issues

A. J. Stoltz, J. D. Benson, P. J. Smith

U.S. Army RDECOM CERDEC Night Vision and Electronic Sensors Directorate, Ft. Belvoir, VA

**Keywords:** ICP, OES, Hydrogen, Photovoltaic, HgCdTe

### Abstract

**Inductively coupled plasmas (ICP) are the high density plasmas of choice for the processing of HgCdTe and related compounds. Real time examination of the ICP plasmas used to process HgCdTe would be desirable. In this preliminary study, the feasibility of using optical emission spectroscopy (OES) with ICP plasma for the processing of HgCdTe will be examined. We will examine the utility of OES as a real time diagnostic tool for HgCdTe device fabrication.**

**In this preliminary study it has been found that mercury and cadmium can be detected but are dependent on several factors: sample area, material x-value, etch rate, sample temperature, photoresist area, and plasma power. Further we found a strong correlation between the amount of hydrogen detected by OES with samples that have photoresist versus samples without photoresist while processing with hydrogen based plasmas. Hydrogen emission intensity decreases dramatically in samples with photoresist and is converse to the theory that photoresist adds hydrogen to the plasma effluent.**

**It appears that hydrogen is complexing with photoresist and reducing the global amount of hydrogen during a process. Further this phenomena may help explain macroloading issues where additional photoresist area slowed HgCdTe, CdTe, and photoresist etch rates.**

### INTRODUCTION

To fabricate advanced multi-color infrared focal plane arrays (IRFPAs) and avalanche photodiodes, trenches exceeding 15  $\mu\text{m}$  in depth with widths limited to 3  $\mu\text{m}$  must be etched into HgCdTe epilayers. To produce these high aspect-ratio profiles, plasma processing is necessary. The exact geometries of these delineations are predominantly affected by photoresist geometry, plasma chemistry, and material properties, and are often complicated by strong interactions between the three. How the plasma interacts with the epilayer film, such as HgCdTe etch rate, the etched epilayer's surface chemistry and surface structure has been previously studied<sup>1-14</sup>. However, little research has been performed to directly examine the HgCdTe plasma gases. In this work, a new to HgCdTe technique, Optical Emission Spectroscopy (OES), will be used to examine the ICP HgCdTe plasma etch gases.

OES allows for real time monitoring of the gases in a plasma without interfering with the process itself. In this paper we will examine the potential of using OES as a possible endpoint detection method as a replacement for an etch stop. We will also examine the effects that different x-values of  $\text{Hg}_{1-x}\text{Cd}_x\text{Te}$  have on OES spectra.

Small changes in ICP plasma gases can drastically impact HgCdTe processing. The plasma etch rate of the epilayer and photoresist mask has been shown to be dependent on wafer area<sup>17</sup>. This effect, known as macro-loading, seriously impacts HgCdTe manufacturing reliability. It will be shown in this paper that OES aids in understanding the area dependence of photoresist and epilayer etch rates. It has been found that in hydrogen based plasmas that increasing photoresist area decreases the global amount of hydrogen in a plasma. This knowledge enables real time changes to be made to ICP plasma parameters for better control of HgCdTe device processing and enables sample scaling issues to be addressed.

### EXPERIMENTAL

A Versaline Unaxis ICP was used for the ICP plasma processing described in this paper. The RF coupled dc bias source is driven at 40.68 MHz, and the primary inductor is driven at 2 MHz. The sample cooling chuck handles 3-inch wafers and was varied between -40 °C and 25 °C with 3 Torr of backside He cooling. The 3-inch sample chuck can be exchanged with an 8 inch chuck for processing larger wafers. The gas input flow mixtures employed for these experiments were 4:1 or 1:0 noble gas/hydrogen by volume. Noble gases, either argon or xenon, are injected into the plasma zone, while the hydrogen is injected downstream of the plasma.

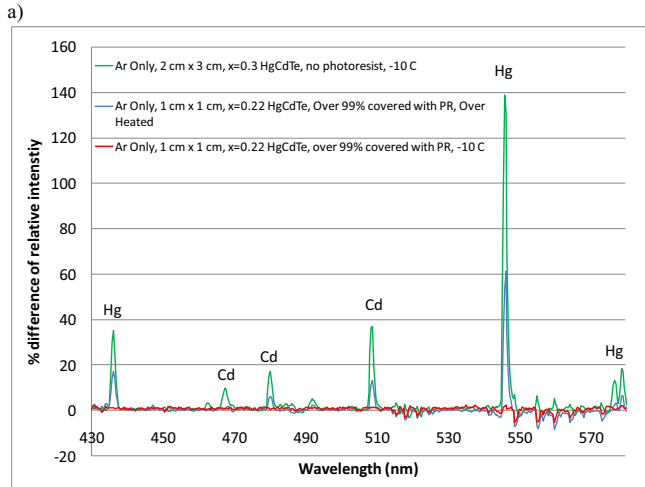
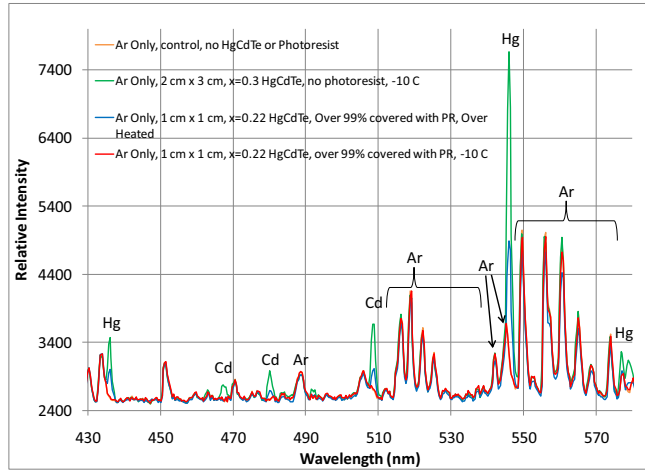
An Ocean Optics USB4000-UV-VIS blaze grated spectrometer was used to perform the optical emission spectroscopy of the plasma. Examples of non-invasive characterization techniques can be found in ref 18. A review of the optical emission spectroscopy technique can be found in ref 19.

### DISCUSSION AND RESULTS

In order to determine if OES can be used for end point detection the question is asked: Can residuals from HgCdTe be detected? Figure 1a contains OES spectra from four widely varying samples that were plasma processed and the OES spectra during processing were examined. Three of these samples have HgCdTe and the fourth, acting as a control, contained no HgCdTe. For all four sample runs, an Ar only plasma utilizing identical processing conditions was used.

One potential problem that can be quickly elucidated from figure 1a is that the plasma gases, in this case Argon, have several emission peaks. Ar has several emission lines between 510 and 580 nm. In contrast, a major peak of interest for Hg detection is the Hg 546 nm emission line. An Ar emission line also exists at 545 nm and can interfere with detection of the Hg 546 nm peak. By examining the difference between the samples with HgCdTe and the control sample (without HgCdTe), Hg and Cd lines can be easily extracted from the background with minimal Ar interference, figure 1b. Luckily most OES systems have software tools that allow integration over reduced wavelength ranges of the OES

spectra and can detect small differential changes in the signal in real time. These algorithms can be used to detect different emission lines even when these spectra overlap with the background plasma gases.



b) Figure 1.a) Optical emission spectra for Ar only processed HgCdTe Test samples b ) intensity difference between samples with HgCdTe, and photoresist normalized on an Ar only processed Si wafer. Ar only plasma used to test low etch rates.

Another potential problem is the detection of HgCdTe. From both figures 1a and 1b the Hg and Cd emission line can be easily detected from two of the HgCdTe samples, but not from the third sample. The first sample with the largest Hg and Cd signals is a  $2 \times 3 \text{ cm}^2$   $\text{Hg}_{0.7}\text{Cd}_{0.3}\text{Te}$  sample mounted on Si. This sample has no photoresist and the sample temperature was controlled to  $-10 \text{ }^\circ\text{C}$  during plasma etching. As exhibited in figure 1a and b, both the Hg and Cd peaks are well defined and detectable. The difference in Hg 546 nm line peak is  $\sim 140\%$  above the control sample background. The second sample was a much smaller  $1 \times 1 \text{ cm}^2$   $\text{Hg}_{0.78}\text{Cd}_{0.22}\text{Te}$  sample. The sample is predominantly covered with photoresist with  $<1\%$  of the sample area non-photoresist coated HgCdTe.

Like the first sample, the Hg and Cd peaks are well defined and are both detectable. For this sample, the difference in the Hg 546 nm line is over  $60\%$  greater than the control sample. However, this

sample did not have good backside helium seal. This resulted in the photoresist just starting to polymerize from overheating during the plasma etching process.

The third sample was a  $1 \times 1 \text{ cm}^2$   $\text{Hg}_{0.78}\text{Cd}_{0.22}\text{Te}$  mounted on Si and processed identically to the 2<sup>nd</sup> sample. In this case, however the sample was properly backside He sealed to the chuck and maintained a temperature of  $-10 \text{ }^\circ\text{C}$  during plasma processing. In this case no changes relative to the control sample could be detected.

As demonstrated in the above experiments the OES spectra is a sensitive technique for studying HgCdTe plasma etching. The change in Hg:Cd ratio also suggests that OES may be able to detect different x-values of HgCdTe. However, x-value, sample area, photoresist area, plasma power, and sample temperature can affect the emission intensity of residual Hg and Cd spectral lines. With the appropriate samples OES may be a useful process monitoring tool for the plasma processing of HgCdTe.

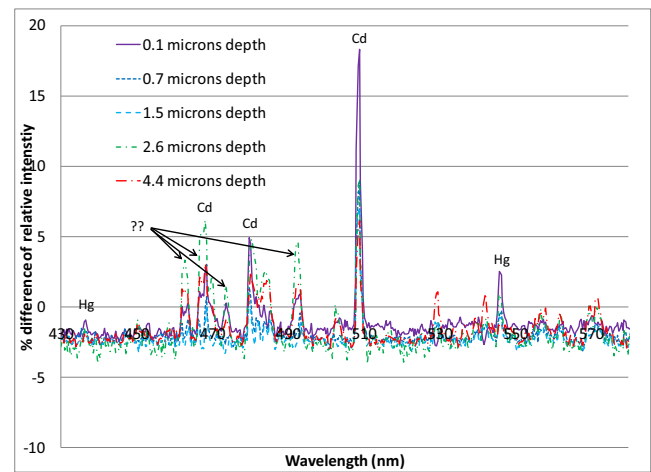


Figure 2. Intensity difference between samples with HgCdTe, photoresist and plain Si wafer. Xe only,  $1 \text{ cm} \times 0.5 \text{ cm}$ ,  $x=0.7 \text{ HgCdTe}$ ,  $\sim 1\%$  covered with PR, Mesa Pattern,  $-10 \text{ }^\circ\text{C}$  temperature.

It has been established that at least in some circumstances, HgCdTe effluent can be detected by OES. However, can high x-value material be detected? And, what happens to a sample over time as a process proceeds? A shortwave infrared  $\text{Hg}_{0.3}\text{Cd}_{0.7}\text{Te}$  sample was processed using a Xe only plasma and the OES spectra examined, figure 2. Few general differences could be detected between the control sample (no HgCdTe material present) and the HgCdTe sample in this figure. The first issue with OES detection of HgCdTe in this sample is the lack of Cd and Hg effluent that can be detected by the OES as compared to samples 1 and 2 in figure 1a and 1b. This is due to the low etch rate that high x-value HgCdTe has as compared to long wavelength HgCdTe. Further the sample was only  $0.5 \text{ cm}^2$  in area. However even with the slow etch rate and the small sample, the Cd and Hg emission signal is still detectable. Further the OES spectra of this  $x=0.7$  short wavelength sample shows emission differences in the the Hg 546 nm line and the Cd 509 nm line have a ratio of approximately 0.2:1. The greater Cd signal relative to the Hg peak is reasonable for this high x-value sample as compared to the 3.8:1 for the  $\text{Hg}_{0.7}\text{Cd}_{0.3}\text{Te}$  and the 5.1:1  $\text{Hg}_{0.78}\text{Cd}_{0.22}\text{Te}$  found in figure 1. As discussed earlier these changes in ratios suggest that OES can be used to detect different x-values of HgCdTe.

What happens to the OES over time? Initially the Hg and Cd signals spike at the initiation of the process. During further etching the signal drops after the initial surface spike. This spike could be related to aggressive plasma ignition. Cd and Hg can be detected deep into the etch HgCdTe but appear to decrease with increasing etch depth. More investigation is needed to fully understand the phenomenon to allow this technique to be useful as an etch stop indicator. In figure 2 there are some difference peaks not detected in the earlier experiments. However, this may be residual Xe signal from the control subtraction algorithm used to process this data.

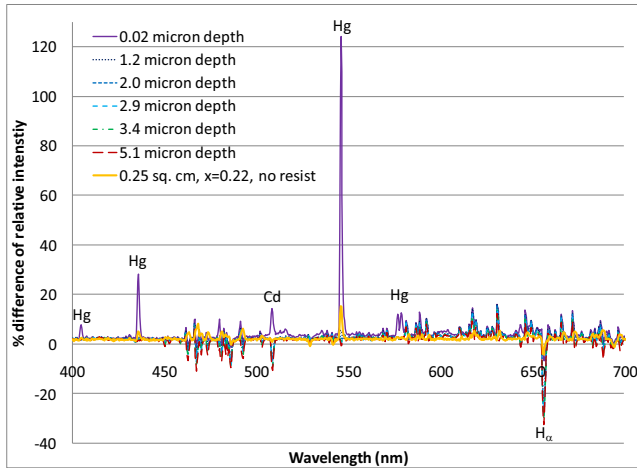


Figure 3. Intensity difference between samples with HgCdTe, photoresist and plain Si wafer. Xe H<sub>2</sub> 4:1, 2 cm x 2 cm, x=0.22 HgCdTe, over 99% covered with PR, Via Pattern, -40 C temperature. Xe H<sub>2</sub> 4:1, ~0.25 cm<sup>2</sup>, x=0.22 HgCdTe, no PR, -10 C temperature, ~0.5 etch depth.

More examination of the OES emission as a function of time during a process is required. Therefore a 2 cm x 2 cm Hg<sub>0.78</sub>Cd<sub>0.22</sub>Te via pattern was plasma-processed with Xe/H<sub>2</sub> based plasma, and the results exhibited in figure 3. The process gases in this experiment are much closer to a standard etch process used to make devices as the etch rate is higher than that shown in figures 1 and 2<sup>15</sup>. Also the sample has photoresist with a pattern representative of a real test device. The sample is mostly covered with photoresist with; less than <1% of the sample is non-photoresist covered HgCdTe. The long wavelength cutoff and therefore Hg content is similar to the samples processed in figure 1. The process was monitored over time with OES. Much like the shortwave sample in figure 2, the Hg and Cd emission spiked at the onset of etching probably due to the aggressive ignition condition. However no Hg can be detected after the initial surface is etched. A small HgCdTe sacrificial area may be needed for deep via etching. To test this hypothesis a small 0.25 sq. cm. Hg<sub>0.78</sub>Cd<sub>0.22</sub>Te sample with no photoresist was also processed using identical process parameters and the results are also exhibited in figure 3. After ~1.0 microns of HgCdTe were removed there is still enough Hg for the 546 nm line to be detected. Not surprisingly the ability of the OES to detect HgCdTe effluent is greatly dependent on sample area. Sufficient non-photoresist coated HgCdTe area is required in order to be detected by OES. This could potentially be a problem with small experimental samples. It is clear that the work presented here is preliminary and further study is needed especially if this technique is used for manufacturing process monitoring.

Another unexpected phenomenon was measured in this process. As observed in figure 3, the difference in the H<sub>α</sub> line between the via etch sample and the control sample is negative 37%. This data shows that 37% less hydrogen signal was detected in the via etch process than in the control process. In the next experiment we will further discuss this decrease in hydrogen.

The HgCdTe sample processed in figure 3 had a significant amount of photoresist covering the sample surface. An experiment was devised to examine the effect that photoresist has on the nobel/hydrogen plasma process used in figure 3. In order simplify the experiment and to examine only the effects photoresist has on the nobel/hydrogen process, four silicon samples without any HgCdTe were etched. The samples had 0 cm<sup>2</sup>, 6.7 cm<sup>2</sup>, 13.5 cm<sup>2</sup>, and 26.8 cm<sup>2</sup> of photoresist coated area. Each was processed and the OES examined. The results of these experiments are shown in figure 4 with the sample containing no photoresist as the control.

Unlike some of the issues of detecting Hg or Cd signals by OES, the hydrogen signal is quite strong as it is one of the main constituents in the plasma. Hydrogen spectral intensity decreases dramatically as shown in figure 4. The change in hydrogen emission from no photoresist to 6.7 cm<sup>2</sup> and from 6.7 cm<sup>2</sup> to 13.5 cm<sup>2</sup> of photoresist is large while the change from 13.5 cm<sup>2</sup> to 26.8 cm<sup>2</sup> was relatively small. Not only was there a large change, but it is consistent across several Hydrogen peaks, H<sub>α</sub>, H<sub>β</sub>, and H<sub>γ</sub>. This result is contrary to what we initially expected which was that as photoresist is etched, hydrogen effluent would be added to the plasma and thus increase the hydrogen signal. It appears that hydrogen is complexing with photoresist and reducing the global amount of hydrogen during the plasma etching process.

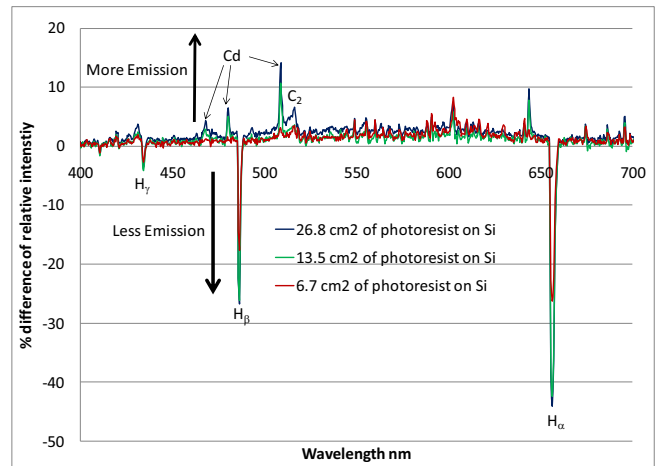


Figure 4. Intensity difference between samples with photoresist and samples without photoresist. No intention HgCdTe used. Ar / H<sub>2</sub> 4:1 gas ratio

As discussed in reference 17, macro-loading exists in the nobel/hydrogen plasma processing of HgCdTe. The macro-loading phenomenon (shown in figure 5) occurs when a global change to the plasma process is made by varying the geometry of the processed sample. Typically either a reactive gas is used up or large volume of effluent is added to the plasma resulting in a global change in the plasma process. From reference 17 one of the major factors affecting macro-loading in HgCdTe is photoresist area. These new hydrogen results may help explain macroloading issues where additional photoresist area slowed HgCdTe, CdTe, and photoresist etch rates. These new results also explain the decrease

in lateral photoresist etching as total photoresist area is increased, shown in figure 5. Hydrogen ions with a high ion angular distribution effect have an primarily effect the etch rate of photoresist<sup>6</sup>.

Also, shown in figure 4, is that the Cd signal increases with photoresist area. This Cd signal increase may be due to hydrocarbon effluent coming from the photoresist. This hydrocarbon effluent may aid in the volatilization of Cd from the chamber walls as no intentional Cd was present on these silicon samples<sup>8-10,14-15</sup>.

Changes in the global hydrogen level as a function of photoresist area may not be the only contributor to the macro-loading effect. As discussed in reference 17, the II-VI semiconductor area may also cause macro-loading changes. The results in this paper could certainly help explain some of the macro-loading found in the plasma processing of HgCdTe and CdTe, but more research is needed for a full explanation. OES spectral analysis has been demonstrated to be a useful technique to resolve macro-loading mechanisms in HgCdTe and related compound semiconductors.

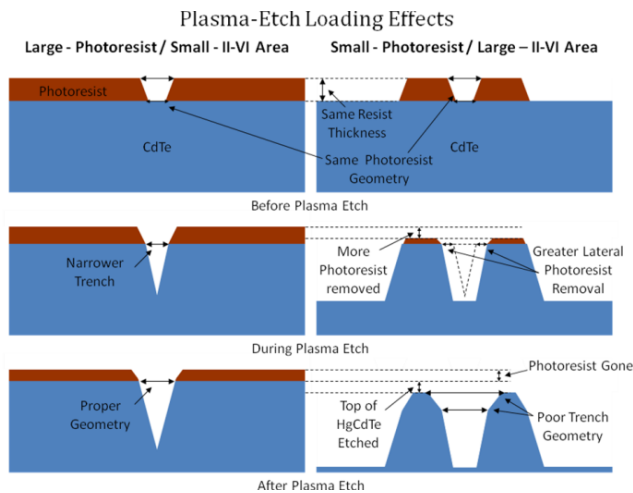


Figure 5. Example of macro-loading effect as measured in reference 17.

## CONCLUSIONS

Optical Emission Spectroscopy (OES) can be used to detect plasma etch parameters in HgCdTe and related II-VI layers. Mercury and cadmium spectral emission lines can be detected but are dependent on many things: sample area, x-value, etch rate, sample temperature, photoresist area, and plasma power. Further, OES has been used to determine that in hydrogen-based plasmas hydrogen emission intensity dramatically decreases with increasing photoresist area. The hydrogen decrease may help explain the macro-loading phenomenon in the plasma processing of HgCdTe measured in earlier papers.<sup>17</sup>

In the future we hope to demonstrate CdTe/HgCdTe end point detection using the OES technique. We hope to form metallization vias in CdTe passivation and etch to expose active HgCdTe device material. We would also like to perform area effect experiments with the plasma processing of HgCdTe and use OES to further examine causes of the macro-loading.

## REFERENCES

[1] P. O'Dette, G. Tarnowski, V. Lukah, M. Krueger, and P. Lovechhip, J. Electron. Mater. 28, 821 (1999).

[2] E. P. G. Smith, L. T. Pham, G. M. Venzor, E. M. Norton, M. D. Newton, P. M. Goetz, V. K. Randall, A. M. Gallagher, G. K. Pierce, E. A. Patten, R. A. Coussa, K. Kosai, W. A. Radford, L. M. Giegerich, J. M. Edwards, S. M. Johnson, S. T. Baur, J. A. Roth, B. Nosh, T. J. DeLyon, J. E. Jensen, and R. E. Longshore, J. Electron. Mater. 33, 509, (2004).

[3] J. Baylet, O. Gravrand, E. Laffosse, C. Vergnaud, S. Ballerand, B. Aventurier, J. C. Deplanche, P. Ballet, P. Castelein, J. P. Chomonal, A. Million, and G. Destefanis, J. Electron. Mater. 33, 690, (2004).

[4] E. P. G. Smith, E. A. Patten, P. M. Goetz, G. M. Venzor, J. A. Roth, B. Z. Nosh, J. D. Benson, A. J. Stoltz, J. B. Varesi, J. E. Jensen, S. M. Johnson, and W. A. Radford, J. Electron. Mater. 35, 1145 (2006).

[5] A. J. Stoltz, J.D. Benson, Mason Thomas, P.R. Boyd, M. Martinka, and J.H. Dinan, J. Electron. Mater. 31, 749 (2002)

[6] A. J. Stoltz, J. D. Benson, P. R. Boyd, J. B. Varesi, M. Martinka, A. W. Kalezcyc, E. P. Smith, S. M. Johnson, W. A. Radford, and J. H. Dinan, J. Electron. Mater. 32, 692, (2003).

[7] E. P. G. Smith, J. K. Gleason, L. T. Pham, E. A. Patten, and M. S. Welkowsky, J. Electron. Mater. 32, 816, (2003).

[8] R. C. Keller, H. Zimmerman, M. Seelmann-Eggebert, and H. J. Richter, J. Electron. Mater., 25, 1270 (1996)

[9] R. C. Keller, H. Zimmerman, M. Seelmann-Eggebert, and H. J. Richter, Appl. Phys. Lett., 67, 3750 (1995)

[10] R. C. Keller, H. Zimmerman, M. Seelmann-Eggebert, and H. J. Richter, J. Electron. Mater., 26, 542 (1997)

[11] C. R. Eddy, Jr., D. Leonhardt, V. A. Shamamian, J. R. Meyer, C. A. Hoffman, and J. E. Butler, J. Electron. Mater., 28, 347 (1999)

[12] A. J. Stoltz, M. J. Sperry, J. D. Benson, J. B. Varesi, M. Martinka, L. A. Almeida, P. R. Boyd, and J. H. Dinan, J. Electron. Mater. 34, 733 (2005).

[13] A. J. Stoltz, M. Jaime Vasquez, J. D. Benson, J. B. Varesi, and M. Martinka, J. Electron. Mater. 35, 1461 (2006).

[14] E. Laffosse, J. Baylet, J. P. Chamonal, G. Destefanis, G. Cartry, and C. Cardinaud, J. Electron. Mater. 34, 740 (2005).

[15] A. J. Stoltz, J. D. Benson, J. Electron. Mater. 36, 1007 (2007).

[16] M. Elwenspoek and H. V. Jansen, Silicon Micromachining (Cambridge, United Kingdom: Cambridge University Press, 1998), PP. 213-233

[17] A. J. Stoltz, J. D. Benson, J. B. Varesi, M. Martinka, A. W. Kalezcyc, L. A. Almeida, P. R. Boyd and J. H. Dinan "Macro-Loading Effects of ECR-Etched II-VI Materials," J. Elec. Mat 33(6) 684, (2004).

[18] F. F. Chen and J. P. Chang, Lecture Notes on Principles of Plasma Processing, Kluwer Academic, New York, 2003.

[19] S. Gershman and A. Belkind, "Plasma Diagnostics Part 2 Optical Emission Spectroscopy," Vacuum & Coating Technology Vol 10, No. 8, August 2009, pp. 38-47.

## ACRONYMS

ICP: Inductively Coupled Plasma  
OES: Optical Emission Spectroscopy